Adsorption assisted desorption of NH_3 on γ-alumina studied with positron emission profiling

D.P. Sobczyk[a], J.J.G. Hesen[a], J. van Grondelle[a], D. Schuring[a], A.M. de Jong[b,*], and R.A. van Santen[a]

[a]*Schuit Institute of Catalysis, Laboratory of Inorganic Chemistry and Catalysis, Eindhoven University of Technology, P.O. Box 513, 5600 MB Eindhoven, The Netherlands*

[b]*Department of Applied Physics, Centre of Plasma and Radiation Physics, Eindhoven University of Technology, P.O. Box 513, 5600 MB Eindhoven, The Netherlands*

Received 19 June 2003; accepted 28 January 2004

Evidence for adsorption assisted desorption of $^{13}NH_3$ in the presence of gas phase ammonia on γ-alumina is presented. Due to lateral interactions with physisorbed ammonia, the adsorption enthalpy of ammonia on γ-alumina was measured to be -11 ± 1 kJ/mol, using a $^{13}NH_3/^{14}NH_3$ isotopic exchange method. This adsorption/desorption exchange was monitored with positron emission profiling. Infrared spectroscopy showed ammonia to exchange preferentially on the Lewis acid sites of alumina.

KEY WORDS: $^{13}NH_3$; labelled ammonia; positron emission profiling; adsorption assisted desorption (AAD); ammonia adsorption; γ-alumina.

1. Introduction

Adsorption assisted desorption (AAD) has become a well-known phenomenon in catalysis [1–6]. According to Boudart [7], AAD describes a desorption step which is not equilibrated, due to a higher concentration of the desorbing surface species than its equilibrium value. The adsorption step lowers the potential energy, that has to be overcome by molecules to desorb, thus facilitating the desorption process. Overall, it results in an increased rate of desorption. The effect of surface coverage (θ) on the rate of desorption explains quantitatively recent data on AAD phenomena. Monte Carlo simulations of the AAD processes ascribed the lowering of the activation energy for desorption to repulsive lateral interactions between the adsorbates [8]. In the present study of ammonia adsorption on γ-alumina, it is revealed that the rate of desorption of ammonia is increased by the gaseous pressure. Desorption of ammonia from alumina proceeds according to the AAD mechanism.

Aluminas are commonly used as acid catalysts and as support material for catalysts. The motivation for this study was to understand the influence of the alumina support on ammonia adsorption in the ammonia oxidation reaction over Pt/γ-alumina. This paper describes for the first time AAD phenomena in which ammonia is involved. Furthermore, AAD has not been reported earlier on alumina. In contrast to Boudart's interpretation [7] our results indicate that the desorption is equilibrated. This may be due to more realistic reaction conditions (1 bar) compared to those reported in literature (ultra high vacuum).

* To whom correspondence should be addressed.
E-mail: A.M.de.Jong@tue.nl

The first indications for AAD were found by Yates and Goodman [9] in a study of CO adsorption on Ni(100). Later, Tamaru and co-workers [1] also showed that the rate of desorption of $C^{18}O$ in the presence of $C^{16}O$ in the gas phase was faster than in vacuum or in the presence of argon. This group investigated this phenomenon for CO on rhodium polycrystalline surfaces [2], and for CO on ruthenium single crystal surfaces [3]. By then, it was revealed that the absolute desorption rate increased with rising CO pressure and the phenomenon AAD was born. Tamaru [4,5] proved that the effect of AAD is to lower the activation energy of desorption by an appreciable amount. The rapid process of AAD seemed to occur on all group VIII metal surfaces, but Sushchikh *et al.* [10] showed that AAD could be excluded for CO on Ir(111) surfaces. Nowadays, the AAD process is recognised and understood. Tracer exchange experiments played a key role in the recognition of the AAD process, which also form the basis of our study.

A suitable technique to study transient and steady state phenomena using tracer exchange is positron emission profiling (PEP) [11–13]. Here we use ^{13}N–labelled ammonia ($^{13}NH_3$). This makes it possible to study the adsorption/desorption rate of $^{13}NH_3$ in a stream of $^{14}NH_3$ on γ-alumina:

$$^{13}NH_{3(g)} \leftrightarrow {}^{13}NH_{3(a)}$$
$$^{13}NH_{3(a)} + {}^{14}NH_{3(g)} \leftrightarrow {}^{13}NH_{3(g)} + {}^{14}NH_{3(a)}.$$

Ammonia adsorption sites of γ-alumina have been identified with infrared (IR) spectroscopy and with temperature programmed desorption (TPD) experiments. The TPD experiments are performed to determine the amount of chemisorbed ammonia at temperatures of 323–473 K. The amount of physisorbed

1011-372X/04/0400–0037/0

ammonia is calculated from the PEP experiments at these temperatures. The evidence for AAD of ammonia on γ-alumina is directly visible with PEP-pulse experiments. In addition, ΔH_{ads} for the AAD process is calculated from the retention times of $^{13}NH_3$ in the reactor in a $^{14}NH_3$/He flow.

2. Experimental

2.1. Characterisation of alumina

A Ketjen E-000 γ-alumina sample was used. The particle size of the samples was 250–425 μm. The surface area of 180 m^2/g and average pore diameter of 110 Å were measured with the B.E.T. method using a Micromeritics TriStar 3000 setup. The iron contamination in the pure γ-alumina was determined to be 0.015 ± 0.001 wt%, using Inductively Coupled Plasma Optical Emission Spectrometry (ICP-OES).

2.2. IR experiments

IR experiments were performed using a Bruker IFSv 113 FTIR spectrometer equipped with a heated vacuum cell. The spectra were recorded by measuring 125 scans at a resolution of 4 cm, using a DTGS detector. The sample was dried in the setup in vacuum at 673 K for 2 h. Ammonia was adsorbed at a pressure of 400 Pa for 30 min at 373 K. Then, the samples were evacuated for 30 min at 373, 473, 573 and 673 K, and spectra were recorded each time at 373 K. It is assumed that physisorbed ammonia is not present on an evacuated γ-alumina.

2.3. Temperature programmed desorption

First the catalyst was heated from 273 K to 403 K in a 10 vol% hydrogen/helium flow of 40 cm^3/min (STP) at a rate of 10 K/min and kept at this temperature for 1 h before raising the temperature by 10 K/min to 653 K. The catalyst was kept at this temperature overnight. The catalyst was then pre-saturated at temperatures of 323–473 K and a pressure of 1 atm with pure ammonia or ammonia in a 1.0 vol% ammonia/helium flow of 48 cm^3/min (STP) for 1 hour. Afterwards, the flow was changed to a helium flow of 33 cm^3/min (STP) and after 20 h the temperature was raised by 5 or 10 K/min to 673 K. The ammonia desorption was monitored by a calibrated quadrupole mass spectrometer (Balzers Instruments Omnistar GSD 3000).

2.4. Positron emission profiling

The Eindhoven 30 MeV cyclotron was used to irradiate water with highly energetic protons of 16 MeV. In this way formed [^{13}N]nitrate and [^{13}N]nitrite were reduced to $^{13}NH_3$, using DeVarda's alloy method [14,15]. The production method of gaseous pulses of [^{13}N]NH_3 was described elsewhere [16]. A pulse time of 5 s was used to inject the radiolabelled gaseous ammonia into the He or $^{14}NH_3$/He stream. The concentration of radiolabelled ammonia was circa 40×10^{-12} mol/L.

Unstable nuclei like ^{13}N, emit a positron upon decay. PEP is based on the detection of the two 511 keV γ-photons which originate from the annihilation of a positron with an electron. These two 511 keV γ-photons are simultaneously emitted in opposite direction and travel typically a few centimetres in solid matters. Coincidental detection of the two photons by scintillation detectors (BGO) provides the position of the annihilation. In practice, the tubular reactor is placed in between 18 scintillation detectors. In this way, the concentration distribution of radiolabelled molecules can be measured as a function of position and time [11,12].

2.5. Ammonia adsorption/desorption PEP experiments

In the PEP-experiments the length of the catalyst bed was 4 cm, and the catalyst volume equal to 0.5 ML. In all PEP images, the ^{13}N half-life of 9.97 min was taken into account. For the AAD experiments, three main types of PEP-experiments were carried out on the pure γ-alumina, which was pre-treated with a 10 vol% hydrogen/helium flow of 40 cm^3/min (STP) at 673 K overnight.

2.5.1. Equilibrium measurements

The pre-treated γ-alumina catalyst was kept under a 1.0 vol% ammonia/helium flow of 48 cm^3/min (STP). Subsequently a pulse of [^{13}N]NH_3 was injected in this ammonia/helium flow. These experiments were performed at temperatures from 243 to 473 K.

2.5.2. AAD measurements

On the pre-treated γ-alumina catalyst a [^{13}N]NH_3 pulse was adsorbed in He flow of 48 cm^3/min. After 400 seconds, the helium flow was changed to a 1.0 vol% ammonia/helium flow of 48 cm^3/min (STP). These experiments were performed at temperatures from 243 to 473 K.

2.5.3. Influence of the flow rate on adsorption/desorption

The pre-treated γ-alumina catalyst was kept under a 1.0 vol% ammonia/helium flow in the range of 48–144 cm^3/min (STP) at 373 K. Subsequently the [^{13}N]NH_3 pulses were injected at different NH_3/He flow velocities: 48, 96 and 144 cm^3/min (STP).

3. Results and discussion

3.1. IR spectroscopy

The acid sites on γ-alumina for ammonia adsorption are Brønsted hydroxyl groups and uncoordinated alumina Lewis sites [17]. Mainly two Lewis-acidic sites, tri- and penta-coordinated aluminum atoms, are present

on the alumina surface. Six types of Brønsted acidic sites on alumina are recognised [18,19], however they are present in very low quantities [20–22] and can be considered as very weak, because they are not strong enough to donate a proton to pyridine. Ammonia preferentially binds to the Lewis-acidic sites [23,24] via a strong donor–acceptor bond between the nitrogen and the aluminum surface atom.

In figure 1 the IR spectra of adsorbed ammonia on γ-alumina are presented, clearly showing the presence of adsorbed ammonia in a wide temperature range. The peaks at 1267 and 1625/cm are characteristic for adsorbed ammonia on a Lewis site. The lower intensity peaks at 1410, 1450 and 1700/cm are assigned to N–H bending modes [25], corresponding to Brønsted site adsorption. Ammonia present in the form of NH_2^- or NH^{2-} is excluded, since according to Dunken *et al.* [26] the dissociation of ammonia will not take place below 773 K. The N–H bending peaks disappear at 573 K. At this temperature ammonia is still adsorbed at Lewis sites. With increasing temperature the peak at 1267/cm becomes weaker and at 673 K ammonia is no longer adsorbed. It is likely that at higher temperatures ammonia is adsorbed at tri-coordinated aluminum sites, which are the strongest acidic sites on alumina [18,27]. Because of the intense peak at 1267/cm it is concluded that ammonia preferentially adsorbs on Lewis sites.

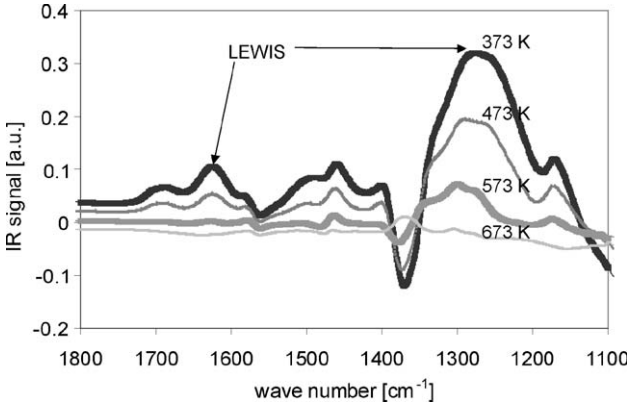

Figure 1. IR spectra of adsorbed ammonia on γ-alumina at 373, 473, 573, and 673 K.

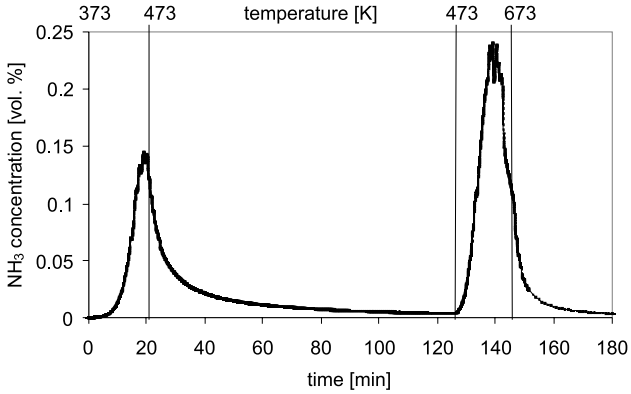

Figure 2. TPD of ammonia with heating rate of 5 K/min from 373 to 473 K and after 2 h, 10 K/min from 473 to 673 K (alumina was pre-saturated with 1 vol% NH_3/He at 373 K).

3.2. Temperature programmed desorption

In a typical TPD spectrum one broad peak of desorbed ammonia is observed in the temperature range of 398–673 K, indicating that re-adsorption of ammonia takes place but also suggests that ammonia adsorbs at different acid sites. This overlap of desorption peaks corresponding to various adsorption states has been observed before [28]. Masuda *et al.* [29,30] also showed that ammonia desorption during TPD experiments is balanced by the adsorption and desorption equilibrium.

On alumina two Lewis sites are present; a weaker Lewis-site attributed to penta-coordinated aluminum atoms (α-type) and a strong Lewis-site with tri-coordinated aluminum atoms (β-site) [18,27]. A TPD experiment is performed in two heating steps as shown in figure 2 to observe the separate peaks of evolved ammonia. A complex TPD spectrum as observed here can also be obtained from a porous material in a packed bed, including re-adsorption coupled with diffusion [31]. Therefore, the qualitative interpretation should be done with caution. Our calculations of dimensionless parameters for a packed bed of Gorte and Demmin [32,33], showed that the transport of ammonia is not diffusion limited, but controlled by an equilibrium in which re-adsorption takes place. The absence of the diffusion limitations indicates that the two separate ammonia peaks observed in the TPD spectrum (figure 2) can be assigned to two acid sites present on the alumina surface (α and β sites). The determined ratio of β/α is 1.2, which is in good agreement with the value of 1.3 reported by van Veen *et al.* [27].

To calculate the ammonia surface coverage, the assumption is made that the maximum coverage of ammonia ($n^{chem}_{ads,max}$) is equal to the chemisorbed amount of ammonia when the γ-alumina surface is pre-saturated with pure ammonia ($p_{NH_3} = 10^5$ Pa). Table 1 presents the amount of desorbed ammonia at pre-saturation of γ-alumina with ammonia (p_{NH_3} is 10^5 and 10^3 Pa) at 323–473 K. The number of ammonia molecules adsorbed on the alumina surface is in good agreement with values reported for the amount of Lewis-acidic sites on γ-alumina [34,35]. At low partial pressure of ammonia ($p_{NH_3} = 10^3$ Pa) the surface coverage is above 90% of maximum surface coverage for temperatures below 423 K. This is due to strong ammonia adsorption on Lewis sites, $k_{ads} > k_{des}$. At higher temperatures less ammonia is chemisorbed and therefore the value for maximum surface coverage is lower. Since different adsorption sites are present on γ-alumina $n^{chem}_{ads,max}$ is strongly dependent on temperature. At higher temper-

Table 1
Amount of ammonia chemisorbed on γ-alumina determined with TPD experiments with pre-saturation with $pNH_3 = 10^5$ Pa ($n_{ads,max}^{chem}$) and $pNH_3 = 10^3$ Pa ($n_{ads}^{chem,p=1000}$) at 323–473 K

Temperature [K]	$n_{ads}^{chem,p=1000}$ [mol/kg]	$n_{ads,max}^{chem}$ [mol/kg]	$n_{ads}^{chem,p=1000}/n_{ads,max}^{chem}$ [%]
323	0.45	0.46	98
373	0.32	0.34	95
423	0.25	0.27	93
473	0.17	0.24	71

atures ammonia preferentially adsorbs on the stronger acid sites. The $n_{ads,max}^{chem}$ value at 473 K mainly originates from the amount of chemisorbed ammonia at β-sites, because ammonia desorbs from the weaker α-site at that temperature as shown in figure 2.

3.3. $[^{13}N]NH_3$ equilibrium pulse experiments

Figure 3 shows a typical PEP-image for a pulse of $[^{13}N]NH_3$ on an ammonia pre-saturated γ-alumina in an ammonia/helium flow. This figure shows that in time the labelled ammonia moves to positions further in the catalyst bed. After 800 s. there is no $^{13}NH_3$ left adsorbed on the alumina, which suggests that only reversible adsorption/desorption took place. Figure 3 also shows that the pulse almost does not broaden while leaving the catalyst bed. This supports the assumption that diffusion limitations are negligible as was already stated in section 3.2.

3.4. $[^{13}N]NH_3$ AAD pulse experiments

Figure 4 shows a typical PEP image for the adsorption/desorption of a labelled pulse of ammonia on γ-alumina in a helium and ammonia/helium flow. In helium flow, $[^{13}N]NH_3$ strongly adsorbs at the beginning of the catalyst bed, because the available amount of acid sites is much higher than the amount of pulsed labelled ammonia. $[^{13}N]NH_3$ remains at the same position in the bed due to its very strong adsorption ($k_{ads} > k_{des}$). In a similar experiment, injection of $[^{13}N]NH_3$ in He flow over a clean γ-alumina surface, it was observed that $^{13}NH_3$ stays at the same bed positions for more than 2000 s. To observe $[^{13}N]NH_3$ desorption and consequent movement of labelled species through the bed temperatures above 600 K were required. Even at these high temperatures the retention time was over 200 min. This result is consistent with the IR and TPD results, $[^{13}N]NH_3$ adsorbs preferentially at the strongest alumina acid sites and desorbs only at relatively high temperatures. This indicates that the adsorption of ammonia on γ-alumina at low temperatures is irreversible.

Figure 4 further shows that after changing the flow to NH_3/He, $[^{13}N]NH_3$ desorbs and travels as a pulse through the reactor. This indicates that $[^{13}N]NH_3$ exchanges rapidly with $[^{14}N]NH_3$. At first sight, this exchange process is very similar to the experiment shown in figure 3. However, in this case radiolabelled ammonia is not in full equilibrium on γ-alumina. After switching to unlabelled ammonia first all the available Lewis sites are saturated. The time to saturate the γ-alumina bed with ammonia, measured with the mass spectrometer at the outlet of the reactor is equal to the retention time of radiolabelled ammonia in the catalyst bed. Thus, the radiolabelled ammonia moves with the saturation front, where ammonia adsorption/desorption is in a kind of quasi equilibrium. We conclude that gas phase ammonia clearly facilitates the desorption of $[^{13}N]NH_3$, it remains adsorbed at the same bed position without ammonia in the gas phase. This proves that AAD takes place for ammonia desorption from γ-alumina.

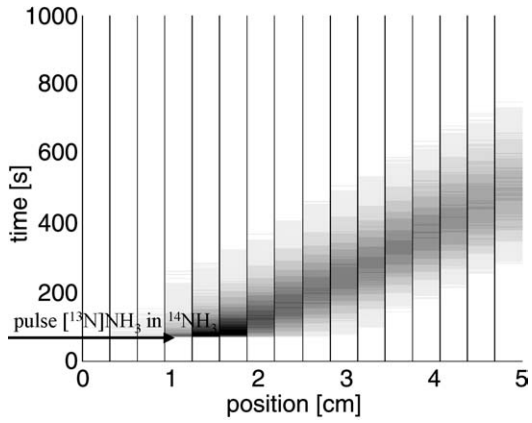

Figure 3. Pulse of $[^{13}N]NH_3$ in a 1 vol% NH_3/He-flow on γ-alumina ($T = 423$ K, $F_t = 48$ cm^3/min, GHSV = 5600 h^{-1}). Colour intensity represents the concentration of $[^{13}N]NH_3$.

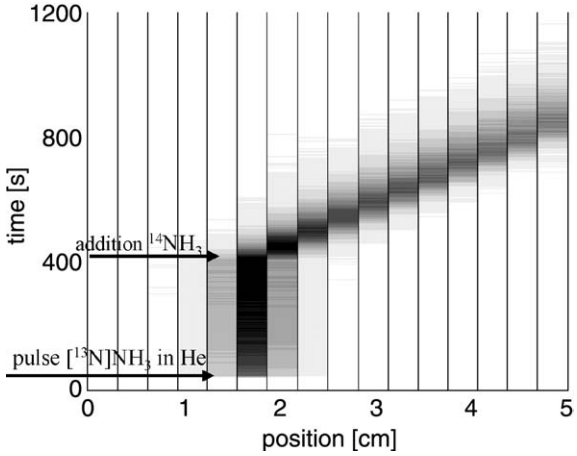

Figure 4. Pulse of $[^{13}N]NH_3$ in a He-flow on γ-alumina. At $t = 400$ s He-flow is changed to 1 vol% NH_3/He-flow ($T = 423$ K, $F_t = 48$ cm^3/min, GHSV = 5600 h^{-1}). Colour intensity represents the concentration of $[^{13}N]NH_3$.

3.5. Determination of ΔH_{ads}

Assuming first order desorption of ammonia, the overall desorption rate can be described by

$$\frac{d\theta_{NH_3}}{dt} = k_{ads}(T) \cdot (1-\theta) \cdot p_{NH_3} - k_{des}(T) \cdot \theta_{NH_3}, \quad (1)$$

where θ_{NH_3} is the surface coverage of ammonia [−], k_{ads} (T) is the adsorption rate constant [1/(Pa · s)], θ is the surface coverage [−], p_{NH_3} is the pressure of gas phase ammonia [Pa], k_{des} (T) is the desorption rate constant [1/s].

Regardless of the form of the rate expression, the mean retention time is given by [36,37]:

$$\mu = \frac{L \cdot \varepsilon}{v} \cdot \left[1 + \left(\frac{1-\varepsilon}{\varepsilon}\right) \cdot K(T)\right], \quad (2)$$

where μ is the retention time [s], L the length of the catalyst bed [m], v the molecular velocity [m/s], ε the porosity of the catalyst bed [−], K(T) the dimensionless equilibrium constant [−].

Equation 2 is used to calculate the K(T). This equation also shows that the retention time is inversely proportional to the flow rate. Table 2 demonstrates that this correlation between retention time and flow rate also applies to the ammonia adsorption equilibrium on the γ-alumina surface, which proves that ammonia adsorption is in equilibrium during our experiments.

Table 2
Retention times of [^{13}N]NH_3 pulse in a 1.0 vol% [^{14}N]NH_3/He flow at variable flow rates of 48, 96 and 144 cm^3/min (STP) at 373 K

Flow rate F [cm^3/min]	Flow rate ratio [%]	Retention time μ [s]	Reciprocal ratio retention time [%]
48	100 (48/48)	695	100 (695/695)
96	50 (48/96)	375	54 (375/695)
144	33 (48/144)	225	32 (225/695)

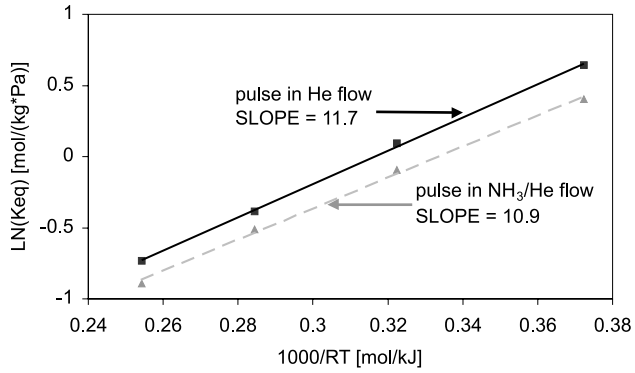

Figure 5. Determination of enthalpy of adsorption (ΔH_{ads}) for ammonia on γ-alumina in the temperature range 323–473 K. Two types of experiments are used: pulse of [^{13}N]NH_3 in ammonia/helium flow (dashed line) and pulse of [^{13}N]NH_3 in helium flow which then is replaced by ammonia/helium flow (solid line).

The dimensional equilibrium constant K_{eq} (T) in [mol/(kg·Pa)], is calculated from

$$K(T) = \rho \cdot R_{gas} \cdot T \cdot K_{eq}(T), \quad (3)$$

where ρ is the density [kg/m^3], R_{gas} the gas constant [J/(mol·K)], T the temperature [K].

The K_{eq} is related to the enthalpy of adsorption and K_{eq} is derived from the van't Hoff equation:

$$K_{eq}(T) = K_\infty \cdot \exp\left(\frac{-\Delta H_{ads}}{R_{gas} \cdot T}\right), \quad (4)$$

where ΔH_{ads} is the isobaric adsorption enthalpy [kJ/mol].

In figure 5 a plot of ln(K_{eq}) versus 1000/RT is presented with the slope equal to $-\Delta H_{ads}$. This figure shows that the values of ΔH_{ads} for both types of PEP-experiments are similar. The average isobaric enthalpy of adsorption is -11 ± 1 kJ/mol for the adsorption of ammonia on γ-alumina. The IR and TPD experiments indicated that the γ-alumina surface is not homogenous, therefore the calculated ΔH_{ads} is an overall value for the adsorption enthalpy. ΔH_{ads} for non-AAD of ammonia is found to be over 50 kJ/mol, as presented in table 3. The significant difference with our value of the heat of adsorption might be subscribed to the effects of lateral interactions, when adsorbed ammonia equilibrates with gas phase ammonia, which causes an increase of the surface coverage. Clearly, in the presence of gas phase ammonia ΔH_{ads} is much lower. Our value is close to the determined ΔH_{ads} by Helminen *et al.* [39], however they calculated an isosteric heat of adsorption.

4. The AAD model

The desorption of ammonia from both Lewis sites is assisted by the presence of gas phase ammonia with a corresponding ΔH_{ads} of −11 kJ/mol. With ammonia in the gas phase the surface coverage increases with a consequent decrease in heat of adsorption. If lateral interactions are involved this affects molecules already present at the surface. We assume that in fact physisorbed ammonia facilitates the desorption of chemisorbed ammonia. The calculated value of the enthalpy of adsorption (−11 kJ/mol) is similar to a heat of vaporisation, which is not surprisingly if one thinks that physisorbed species are involved in the process. The AAD can be described as follows. The physisorption of ammonia takes place on irreversibly chemisorbed ammonia and the ammonia molecules can exchange. Without the presence of physisorbed ammonia chemisorbed ammonia does not desorb. The physisorption of ammonia is equilibrated. The exchange of physisorbed ammonia with chemisorbed ammonia is much faster than the equilibrium constant of the physisorption. A Langmuir type of the physisorption for ammonia is assumed:

Table 3
Values for $E_{act,des}$ and ΔH_{ads} of ammonia on γ-alumina

$E_{act,des}$ [kJ/mol]	ΔH_{ads} [kJ/mol]	Method	Reference
45[a]		Flash-desorption	Amenomiya *et al.* [38]
	−54[a]	Chemisorption (weight measurement)	Dunken *et al.* [26]
	−50[a]	Volumetric adsorption equilibrium	Helminen *et al.* [39]
	$-13.1^{a} \pm 0.8$	Fit of adsorption isotherm with Langmuir–Freundlich-1 (isosteric ΔH_{ads})	Helminen *et al.* [39]
10.0 ± 0.9		Fit of adsorption isotherm with Dubinin–Astakhov model	Helminen *et al.* [39]
	$-11^{a} \pm 1$	PEP experiments (isobaric ΔH_{ads})	This study

[a]The ratio of the number of ammonia molecules per 100 Å^2 of the catalyst is 0.1, assuming the cross sectional area of an ammonia molecule to be 13 Å^2 [38] or 16 Å^2 [24].

$$K_{eq}^{(phys)} \cdot p_{NH_3} = \frac{\theta_{NH_3}^{(phys)}}{1 - \theta_{NH_3}^{(phys)}}, \quad (5)$$

where $K_{eq}^{(phys)}$ is the equilibrium constant for ammonia physisorption [1/Pa], p_{NH_3} is the pressure of ammonia [Pa], $\theta_{NH_3}^{(phys)}$ is surface coverage of physisorbed ammonia.

The equilibrium constant $K_{eq}^{(phys)}$ [1/Pa], is related to K_{eq} (T), which is calculated (equation 3) from the retention times:

$$K_{eq}^{(phys)} = \frac{K_{eq}(T)}{N_T}, \quad (6)$$

where N_T is the number of total adsorption sites, equal to the maximum amount of chemisorbed ammonia ($n_{ads,max}^{chem}$) at the corresponding temperature.

The amount of physisorbed ammonia (n_{ads}^{phys}) during the equilibrium (shown in figure 3) is obtained from the PEP-pulse experiments and n_{ads}^{chem} from the TPD experiments (shown in figure 2). Consistently, $\theta_{NH_3}^{(phys)}$ can be calculated from equation 5.

Table 4 shows the resulting values for experiments performed with 1 vol% of ammonia ($p_{NH_3} = 10^3$ Pa): K_{eq} (T), $n_{ads}^{chem,p=1000}$, $n_{ads}^{phys,p=1000}$ and the ratio $n_{ads}^{phys,p=1000}/n_{ads}^{chem,p=1000}$. As expected K_{eq} decreases with increasing temperature. The ratio $n_{ads}^{phys,p=1000}/n_{ads}^{chem,p=1000}$ is close to unity for all temperatures. For example, the value of 0.79 for $n_{ads}^{phys,p=1000}/n_{ads}^{chem,p=1000}$ at 373 K means that on average almost one molecule of ammonia is physisorbed on one molecule of chemisorbed ammonia.

Table 5 shows the values of K_{eq} (T), $n_{ads}^{chem,p=1000}$, $n_{ads}^{phys,p=1000}$ and $n_{ads}^{phys,p=1000}/n_{ads}^{chem,p=1000}$ obtained from the AAD pulse experiments (figure 4). The retention times are obviously somewhat higher than for experiments carried out on a pre-saturated γ-alumina surface (table 4). The calculated n_{ads}^{phys} is almost equal to the values from the [^{13}N]NH_3 pulse experiments in NH_3/He flow, meaning that the adsorption equilibrium is reached very fast and that the transport of ammonia is controlled by re-adsorption.

5. Conclusions

The adsorption of ammonia on γ-alumina was studied IR, TPD and PEP. IR spectroscopy showed that ammo-

Table 4
Determination of surface coverage from ammonia PEP-equilibrium experiments. A pulse of [^{13}N]NH_3 was injected in [^{14}N]NH_3/He flow of 1 vol%

T [K]	Retention time μ [s]	K_{eq} (T) [10^{-3} mol/kg · Pa]	$n_{ads}^{phys,p=1000}$ [mol/kg]	$n_{ads}^{chem,p=1000}$ [mol/kg]	$n_{ads}^{phys,p=1000}/n_{ads}^{chem,p=1000}$
323	1000	1.50	0.35	0.45	0.78
373	695	0.91	0.25	0.32	0.79
423	520	0.60	0.19	0.25	0.74
473	400	0.41	0.15	0.17	0.89

Table 5
Surface coverage from AAD experiments. A pulse of [^{13}N]NH_3 was injected in a helium flow, then the helium flow was replaced by a [^{14}N]NH_3/He flow of 1 vol%

T [K]	Retention time μ[s]	K_{eq} (T) [10^{-3} mol/kg · Pa]	$n_{ads}^{phys,p=1000}$ [mol/kg]	$n_{ads}^{chem,p=1000}$ [mol/kg]	$n_{ads}^{phys,p=1000}/n_{ads}^{chem,p=1000}$
323	1250	1.9	0.37	0.45	0.82
373	825	1.1	0.26	0.32	0.81
423	585	0.68	0.19	0.25	0.77
473	465	0.48	0.16	0.17	0.94

nia preferentially adsorbs on Lewis sites. Two different Lewis adsorption sites for ammonia were distinguished in a stepped TPD experiment. The ratio determined from the desorption peak areas is calculated to be 1.2. The total amount of chemisorbed ammonia was 0.46 mol/kg at 323 K. These results are comparable with values found in literature and with the fact that on γ-alumina two Lewis sites are mainly present: penta-coordinated aluminum atoms (α-type) and the tri-coordinated aluminum atoms (β-site) [27,34,35].

Radiolabelled experiments, which involved the $[^{13}N]NH_3/[^{14}N]NH_3$ exchange reaction on γ-alumina, showed that AAD of ammonia takes place on γ-alumina. The PEP proved to be a very useful technique to visualise this AAD phenomenon. We observed that a $[^{13}N]NH_3$ pulse adsorbs irreversibly on γ-alumina in a He flow and only desorbs in the presence of ammonia in the gas phase. Further, we assumed that ammonia physisorbs on chemisorbed ammonia and that they exchange. In fact, the exchange between physi- and chemisorbed ammonia is much faster than the physisorption equilibrium. As a result the presence of physisorbed ammonia strongly affects the desorption of chemisorbed ammonia and ΔH_{ads} of chemisorbed ammonia on γ-alumina is lowered. The PEP-technique allowed us to measure the heat of adsorption of ammonia on γ-alumina during the ammonia equilibrium. The overall isobaric heat of adsorption is calculated to be -11 kJ/mol $\pm$ 1 kJ/mol in the temperature range of 323–473 K.

References

[1] T. Yamada, T. Onishi and K. Tamaru, Surf. Sci. 133 (1983) 533.
[2] T. Yamada and K. Tamaru, Surf. Sci. 138 (1984) L155.
[3] T. Yamada and K. Tamaru, Surf. Sci. 146 (1984) 341.
[4] K. Tamaru, Colloids Surf. 38 (1989) 125.
[5] K. Tamaru, Appl. Catal. A 151 (1997) 167.
[6] M. Xu and E.J. Iglesia, Phys. Chem. B 102 (1998) 961.
[7] M. Boudart, J. Mol. Catal. A 141 (1999) 1.
[8] S.J. Lombardo and A.T. Bell, Surf. Sci. 245 (1991) 213.
[9] J.T. Yates Jr. and D.W. Goodman, J. Chem. Phys. 73 (1980) 5371.
[10] M. Sushchikh, J. Lauterbach and W.H. Weinberg, Surf. Sci. 393 (1997) 135.
[11] B.G. Anderson, R.A. van Santen and L.J. van IJzendoorn, Appl. Catal. A 160 (1997) 125.
[12] B.G. Anderson, R.A. van Santen and A.M. de Jong, Top. Catal. 8 (1999) 125.
[13] G. Jonkers, K.A. Vonkeman, S.W.A. van der Wal and R.A. van Santen, Nature 355 (1992) 63.
[14] W. Vaalburg, W.A.A. Kamphuis, H.D. Beerling van der Molen, S. Reiffers, A. Rijskamp and M.G. Woldring, Int. J. Appl. Radiat. Isot. 26 (1975) 316.
[15] K. Suzuki and Y. Yoshida, Appl. Radiat. Isot. 50 (1999) 497.
[16] D.P. Sobczyk, J. van Grondelle, A.M. de Jong, M.J.A. de Voigt and R.A. van Santen, Appl. Radiat. Isot. 57 (2002) 201.
[17] J.B. Peri, J. Phys. Chem. 69 (1965) 220.
[18] H. Knözinger and P. Ratnasamy, Catal. Rev.-Sci. Eng. 17 (1978) 31.
[19] H. Kawakami and S. Yoshida, J. Chem. Soc. Faraday Trans. 2 82 (1986) 1385.
[20] O. Kresnawahjuesa, R.J. Gorte, D. de Oliveira and L.Y. Lau, Catal. Lett. 3 (2002) 155.
[21] A.V. Kiselev and V.I. Lygin, *Infrared Spectra of Surface Compounds* (John Wiley & Sons, New York, 1975).
[22] G. Centi and S. Perathoner, Catal. Rev.-Sci. Eng. 40 (1998) 175.
[23] X. Liu and R.E. Truitt, J. Am. Chem. Soc. 119 (1997) 9856.
[24] H. Knözinger, H. Krietenbrink and P. Ratnasamy, J. Catal. 48 (1977) 436.
[25] J. Medema, J.J.G.M. van Bokhoven and A.E.T. Kuiper, J. Catal. 25 (1972) 238.
[26] H. Dunken, P. Fink and E. Pilz, Chem. Technol. 18 (1966) 490.
[27] J.A.R. van Veen, G. Jonkers and W.H. Hesselink, J. Chem. Soc. Faraday Trans. 1 85 (1989) 389.
[28] Y. Amenomiya, Chem. Technol. 6 (1976) 128.
[29] T. Masuda, Y. Fujikata, H. Ikeda, S. Matsushita and K. Hashimoto, Appl. Catal. A 162 (1997) 29.
[30] T. Masuda, Y. Fujikata, S.R. Mukai and K. Hashimoto, Appl. Catal. A 165 (1997) 57.
[31] R.J. Gorte, Catal. Today 28 (1996) 405.
[32] R.J. Gorte, J. Catal. 75 (1982) 164.
[33] R.A. Demmin and R.J. Gorte, J. Catal. 90 (1984) 32.
[34] Y. Amenomiya, J. Catal. 46 (1977) 326.
[35] J.A.R. van Veen, P.A.J.M. Hendriks, E.J.G.M. Romers and R.R. Andréa, J. Phys. Chem. 94 (1990) 5275.
[36] D.M. Ruthven, *Principles of Adsorption and Adsorption Processes* (John Wiley & Sons, New York, 1984).
[37] J. Kärger and D.M. Ruthven, *Diffusion in Zeolites and Other Microporous Solids* (John Wiley & Sons, New York, 1992).
[38] Y. Amenomiya, J.H.B. Chenier and R.J. Cvetanovic, J. Phys. Chem. 68 (1964) 52.
[39] J. Helminen, J. Helenius, E. Paatero and I. Turunen, AICHE 46 (2000) 1541.